Check for updates

Article

JOURNAL OF COMPOSITE MATERIALS

Journal of Composite Materials
2014, Vol. 48(7) 861–878
© The Author(s) 2013
Reprints and permissions:
sagepub.co.uk/journalsPermissions.nav
DOI: 10.1177/0021998313479416
jcm.sagepub.com
SAGE

Radiation effects on composites for long-duration lunar habitats

Kristina Rojdev[1,2], Mary Jane E O'Rourke[1], Charles Hill[1], Steven Nutt[2] and William Atwell[3]

Abstract

Fiber-reinforced composites are of great interest to NASA for deep-space habitation missions due to the specific strength, modulus and potential radiation shielding properties. However, the durability of these materials on long-duration missions has not been evaluated. Few studies have been conducted on the radiation effects of fiber-reinforced composites in space and even fewer have been conducted with high-energy protons, which replicate portions of the deep-space radiation environment. Furthermore, previous studies of carbon fiber-reinforced composites focused on pure epoxy composites, and aerospace composites in use today include toughening agents to increase the toughness of the material. These toughening agents are typically either rubber particles or thermoplastics, known to be susceptible to ionizing radiation, and could affect the overall composite durability when exposed to high-energy protons. Thus, NASA has undertaken a study to understand the long-term radiation effects on one such potential composite for use in deep-space habitats (boron fiber, carbon fiber and semi-toughened epoxy). Samples were irradiated with 200 MeV protons in air to different doses and evaluated via tensile tests, differential scanning calorimetry, Fourier transform infrared spectroscopy and scanning electron microscopy. The results showed evidence of a weakened matrix due to scission effects and interfacial failure as a result of resin debonding from the boron fibers.

Keywords

Composite, proton radiation, deep space, scission, aging, lunar habitat

Introduction

NASA's exploration goals have focused on deep-space and interplanetary habitation where crew must live and work for extended durations. To accomplish these goals, large structures must be designed to provide a safe environment for crew, and to launch such large structures, they must be strong and lightweight. Thus, fiber-reinforced composites are considered candidate materials for these habitation structures. However, there are few reports on the susceptibility of these materials to aging in the harsh space environment.[1–4]

Milkovich et al.[1] studied a common aerospace composite of the 1980s, T300/934, which contained an untoughened epoxy. Several laminate configurations were investigated and were exposed to 1 MeV electron radiation at a dose rate of 1.8E9 Gy/s to a total dose of 1E8 Gy, simulating a composite in Earth orbit exposed to the Van Allen radiation belts. In addition to the radiation exposure, these samples were subjected to either a cold temperature, room temperature or an elevated temperature to investigate the material properties in the combined thermal and radiation environment. The authors reported that the electron radiation degraded the in-plane strength properties as a result of radiation interaction with the matrix chemistry and noted that this was most severe in laminate configurations that were tested perpendicular to the fiber direction.

Leung et al.[2] also studied T300/934 and exposed the material to gamma radiation of several doses ranging from 4.4E5 Gy to 3.2 E6 Gy (comparable to three years at a geostationary orbit) at a dose rate of 0.714 Gy/s.

[1]NASA-Johnson Space Center, Houston, TX, USA
[2]University of Southern California, Mork Family Department of Chemical Engineering and Materials Science, Los Angeles, CA, USA
[3]The Boeing Company, Seattle, WA, USA

Corresponding author:
Kristina Rojdev, NASA-Johnson Space Center, 2101 NASA Parkway, Houston, TX 77058, USA.
Email: kristina.rojdev-1@nasa.gov; rojdev@usc.edu

The results of this study not only showed the glass transition temperature (T_g) to decrease with radiation exposure, indicating increased molecular mobility of the matrix, but also showed the interlaminar shear strength to initially increase and then decrease back to the original value through the range of doses. The authors did not discuss these results in great detail but only mentioned that longer term radiation exposure would become detrimental to the material, which would seem consistent with the results found by Milkovich[1] at the higher doses studied.

Kurland et al.[3] also studied T300/934 along with T300/5208 and C6000/P1700, and exposed the composites to a simulated geostationary Earth orbit (GEO) radiation environment of 700 keV electrons to doses between 1E7 Gy and 1E8 Gy at a dose rate around 80 Gy/s to 100 Gy/s, again simulating the electron environment in the trapped Van Allen belts. The results showed no significant differences in the composites exposed to radiation compared with the controls, but the trends showed slightly increased stiffness and strength with decreased ultimate elongation. These results indicate matrix crosslinking which contradicts the results suggested in Milkovich's study.[1] Furthermore, Kurland et al.[3] recommended expanding the study to include other types of radiation in the space environment such as high energy protons, low energy charged particles and ultraviolet radiation.

Coulter et al.[4] expanded upon Kurland's[3] work by investigating Narmco 5208 epoxy exposed to 3 MeV protons under vacuum. The doses studied ranged from 5E5 to 1E8 Gy, comparable to the other studies, and the dose rates ranged from 1.5E3 to 2.6E4 Gy/s. Coulter[4] mentioned in his introduction that the mechanisms and results of proton radiation are different than electron radiation because protons are more massive, produce increased ionization density and excitation of atomic electrons and can cause more displacements in materials. The results of this study showed that there were no measureable changes in mechanical properties or Fourier transform infrared (FTIR) spectra. However, UV-visible absorption spectra showed indications of crosslinking and electron spin resonance spectra showed evidence of radical decay species that decayed over weeks, assumed by Coulter to be a recombination of two radicals to form new crosslinks. Coulter's[4] results for Narmco 5208 epoxy are in line with the results from Kurland[3] with T300/5208.

These studies were completed in the 1980s when composites became of interest to NASA for Earth orbit missions and the focus was on Earth orbit environments, primarily the Van Allen radiation belts which contain electrons and protons. The majority of these studies focused on the electron environment in the Van Allen belts and fairly low energies of electrons. NASA is expanding explorations to deep space, in which the radiation environment is quite different from LEO, and includes high-energy protons from solar particle events (SPEs) and very high-energy particles from galactic cosmic rays (GCRs). The studies published to date have not investigated these high-energy, alternate radiation sources, and their impact on the composite materials that might be considered for deep-space habitats. Furthermore, the composites of the 1980s typically featured untoughened polymer matrices. As composite usage has expanded in the aerospace industry, toughening of the matrix has become a standard practice to reduce the brittleness of epoxies, typically through inclusion of either rubber particles or thermoplastics.[5–7] Previous studies of composites in space radiation environments have not considered current state-of-the-art toughened composites. Finally, previous studies on composites for space environments were heavily focused on irradiations in vacuum since the materials were being used as exterior components in Earth orbit. For a deep-space habitat, the interior will be pressurized with air where crews will be living and working, and the habitat will be exposed to higher energies of radiation, which penetrate more deeply than some of the radiation experienced in Earth orbit. If spacecraft designers are to consider using these commercially available composites for the structural components of the habitat, it is necessary to understand how these composites will fare when exposed to high-energy, deep-space radiation in an air environment to determine possible effects arising from interactions with oxygen. The objective of this article is to better understand the durability of candidate habitat composites, consisting of boron and carbon fibers in a semi-toughened epoxy, in a lunar radiation environment.

To broaden the relevance of this study, certain assumptions were made with regard to the environment and the conditions surrounding a lunar habitat. The mission assumptions were that the habitat would be unshielded from radiation on the lunar surface (e.g. not covered with lunar regolith) and remain in service for approximately 30 years. Furthermore, the habitat would be pressurized on the interior, with air at decreased pressure and an elevated oxygen concentration (55.2 kPa (8 psi) and 32% oxygen concentration) for ease of extravehicular activities.

The primary radiation environment on the lunar surface consists of SPEs in accordance with the solar cycle and GCR modulated by the solar cycle. The solar cycle is approximately 11years and contains periods of high solar activity (solar maximum) followed by periods of low solar activity (solar minimum). During solar maximum, there are more SPEs and a higher potential for large SPEs. NASA's Human Integration Design Handbook[8] states that SPE data collected since 1956

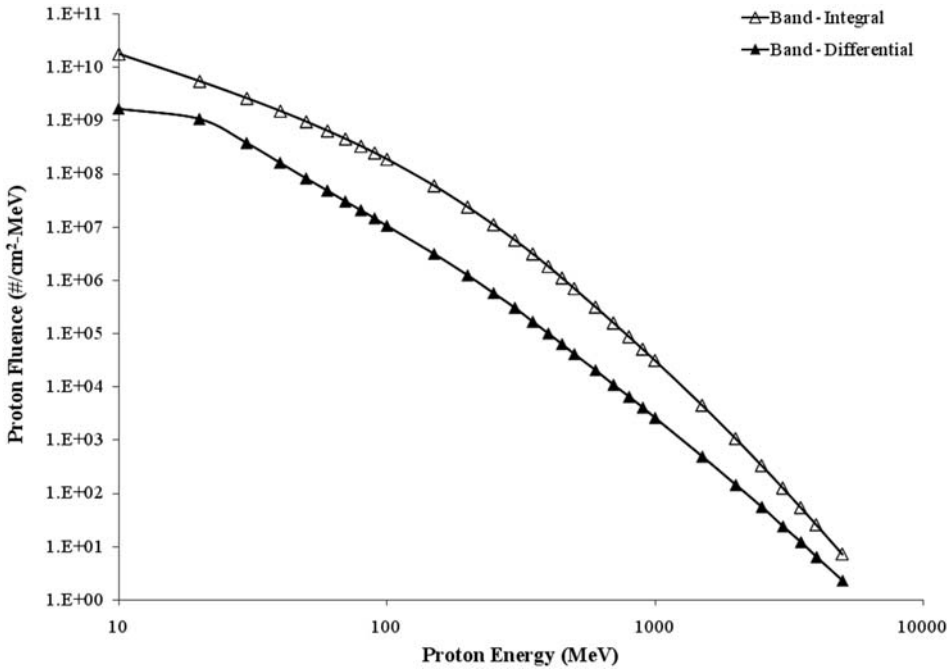

Figure 1. Differential and integral spectra of the band function fit of the combined October 1989 solar particle events.[9]

show '...that about 30 to 50 major SPE events occur per cycle, most during the five years corresponding to solar maximum'. An example of one event that contained a large fluence at very high energies was in October of 1989 (Figure 1), where there was a series of SPEs that occurred on 19, 22 and 24 October.[9] SPEs are composed of about 98% protons and 2% helium.[8]

In contrast, GCRs are high-energy particles originating outside the solar system and are always present, rather than occurring during a short period of time. They are isotropic, consist of 87% protons, 12% alpha particles and 1% heavier nuclei, and are more intense during solar minimum.[8]

Radiation transport calculations/ simulations

To better characterize the radiation environment to which a habitat would be subjected on the lunar surface, preliminary radiation transport calculations were performed using a deterministic high-charge-and energy (HZE) software package (HZETRN). HZETRN is a one-dimensional formulation of the Boltzmann transport equation with a straight-ahead approximation and a continuous slowing-down process.[10] This software contains pre-programmed environments and performs dose calculations very quickly for aid in the design of spacecraft in various radiation environments. For this study, HZETRN was used to investigate the absorbed doses a habitat might experience on the lunar surface when exposed to SPEs and GCRs as described above. The environments selected in these simulations include the October 1989 series of SPEs, 1989 GCR environment during solar maximum and 1977 GCR environment during solar minimum. The GCR environments were arbitrarily chosen and the October 1989 series of events were chosen for the particular large amount of particles at very high energies, as described earlier. The habitat material was simulated in the software by a single slab composed of 24% epoxy, 38% carbon and 38% boron.

The software output provides dose information as if the spacecraft were in free space. Because we are assuming that the habitat is on the lunar surface, half of the dose is removed, reflecting the inherent shielding of the moon, which protects the habitat on one side. Thus, the dose values were divided by two to accurately represent the absorbed dose on the lunar surface. The SPE results are given as a total dose for the entire event since it is a single event, whereas the GCR results are presented as a dose per day, since GCR particles are always present in the background.

In our simulation, the total calculated dose over the five-day October 1989 event to the skin of a habitat material on the lunar surface is approximately 20,000 cGy (1 centiGray [cGy] = 1 rad), at a dose rate of 4.63 E-4 Gy/s (averaged over the five days). In contrast, the skin of a habitat material on the lunar surface over a five-day period during solar minimum (worst case)

receives a GCR dose of approximately 0.07995 cGy at a dose rate of 1.85 E–9 Gy/s (averaged over the five days), which is 200% less dose and subjected to radiation 200% slower than the SPE exposure. Given these values, the majority of the dose a habitat will experience will result from large SPEs that occur throughout the mission. Therefore, it is necessary to simulate SPEs with proton radiation, as 98% of SPEs are composed of protons. The energy profile of the October 1989 SPEs (Figure 1) shows a significant fluence at very high energies and it would be desirable to investigate the effects of these higher energies on the material. Furthermore, we must account for the dose rate in simulation to allow for dose rate effects on the material response.[11–13]

Finally, to calculate the total dose a habitat might receive on the lunar surface over a 30-year mission, the following assumptions were used: one large SPE occurs during each solar cycle, the habitat is subjected to GCR during solar minimum for five years and solar maximum for five years in each solar cycle and a safety factor of 10 is included for any additional SPEs that might occur in each cycle. Based on these calculations, a habitat material would experience approximately 5000 Gy (500 krad) on the lunar surface and 10,000 Gy (1 Mrad) in deep space.

These transport calculations provided the basis for determining the radiation exposure during the experiment. However, simulating the space radiation environment in its entirety is difficult and cost prohibitive. Therefore, certain concessions were required to allow for this type of research. As described earlier, the spectra of SPEs (e.g. Figure 1) or GCRs span a range of energies, and exposing materials over the entire range is cost-prohibitive. In addition, the cyclotron used for the radiation exposures, Indiana University Cyclotron Facility (IUCF), provides proton energies up to 200 MeV. To perform irradiation at a lower energy, a degrader would be required, and this can cause a multitude of secondary radiation. Thus, to preserve the type of primary radiation a habitat would experience in space, we chose to expose the material to 200 MeV protons only.

A 30-year mission will include bursts of radiation over time, but materials will also age with time in addition to the radiation exposure. Ideally, the materials should be exposed to radiation approximately equal to one solar cycle, then aged for an equivalent 11 years and then the procedure repeated twice to arrive at the 30-year exposure. However, this process is both cost and time-prohibitive. Therefore, the radiation exposure was accelerated for practicality, with the 30-year exposure occurring within one day and with no accelerated aging of the material performed.

Material and methods

The material chosen for this study was a unidirectional pre-impregnated composite (Specialty Materials, Inc.)

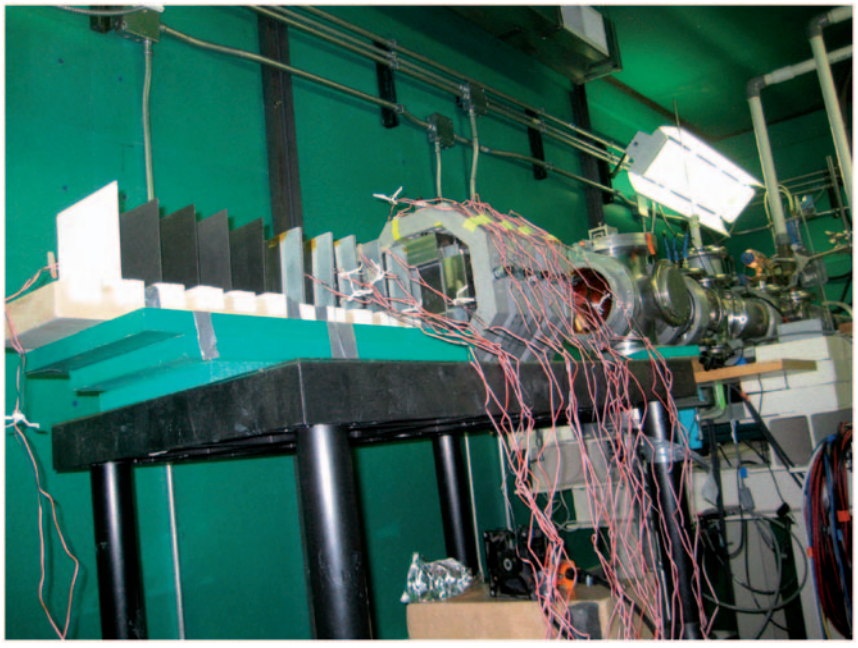

Figure 2. Test setup of stacked configuration of panels at Indiana University Cyclotron Facility prior to radiation exposure.

composed of carbon fibers (CF, MR-40), boron fibers (BF) and a semi-toughened epoxy (Newport 301). The layup design was quasi-isotropic, symmetric and balanced: $[+60/-60/0]_s$. Using this layup, 152.4 mm × 152.4 mm panels were created and cured in a press following the cure cycle specified by the resin manufacturer (16° C/min ramp to 135° C; hold for 60 min, cool to < 60° C). After curing, the panels were inspected ultrasonically and evaluated for defects. Those panels that failed the ultrasonic evaluation were excluded from the study. The panels were then cut down to 139.7 mm × 139.7 mm and the excess material was used for differential scanning calorimetry (DSC) to determine the glass transition temperature (T_g) of the material prior to radiation exposure.

The panels were irradiated under ambient conditions with 200 MeV protons (Indiana University Cyclotron Facility – IUCF) to the following doses: 1000 Gy (100 krad), 5000 Gy (500 krad), 10,000 Gy (1000 krad = 1 Mrad) and 180,000 Gy (18,000 krad). The corresponding fluences are the following: 1.6E15 m^{-2}, 8.36E15 m^{-2}, 1.67E16 m^{-2}, and 3.06E17 m^{-2}. The beam size was 0.07 m and the uniformity was less than 30% variation.[14] Panels were divided into 'fast' exposures (1.973 Gy/s or 197.3 rad/s, and 3.3E12 $m^{-2}s^{-1}$ flux) and 'slow' exposures (0.177 Gy/s or 17.7 rad/s, and 2.95E11 $m^{-2}s^{-1}$ flux), and panels were irradiated in a stacked configuration (Figure 2) at their respective dose rates. The exposure details are shown in Table 1. After radiation exposure, the panels remained at IUCF for two weeks to allow the radioactivity of the panels to decay below regulation limits before safely transporting.

Panels were cut into coupons for tensile testing after irradiation. The tensile coupons were 12.7 cm (0.5 in.) wide and 139.7 cm (5.5 in.) long. The coupons were cut from the panel such that tensile forces were applied perpendicular to the zero-degree ply of the layup to enhance matrix-dominated effects. An axial strain gage was affixed to the center of the coupon to collect strain data during the test. The tensile testing commenced approximately four months after the radiation exposure and followed the procedures outlined in ASTM-D-3039, with the exception of the coupon geometry. The tensile coupons were restricted to above-mentioned dimensions due to limitations of the exposure area. The radiation exposure area was 2827 mm^2 due to the beam size at IUCF. Stress–strain curves were generated from the data and the following properties were measured using the procedures in ASTM-D-3039: modulus, ultimate strength, fracture strength, strain-to-failure, fracture energy and first fracture point. Some of these quantities are shown in the representative graph (Figure 3). The fracture energy is the area under the stress–strain curve and represents the total energy required to break the coupon. The first fracture point is the first point at which the curve deviates from a straight line. Figure 3 is intended for illustration purposes to demonstrate the information gathered from a stress–strain curve. Details of the stress–strain curves are presented in the 'Results and discussion' section.

In addition, two 30 mg samples were cut post-irradiation for DSC analysis. Each sample went through a heat–cool–heat cycle and the results for

Table 1. Exposure details and characterization method for each panel. In the characterization column, T represents tensile test and DSC represents differential scanning calorimetry.

Panel #	Speed	Dose (Gy)	Characterization
BF–CF #56	N/A	0	T
BF–CF #58	N/A	0	T
BF–CF #59	N/A	0	T
BF–CF #60	N/A	0	T
BF–CF #62	N/A	0	T
BF–CF #63-1	N/A	0	T
BF–CF #63-2	N/A	0	T
BF–CF #63-3	N/A	0	T
BF–CF #46	Fast	1000	DSC
BF–CF #61	Fast	1000	DSC
BF–CF #36	Fast	5000	T, DSC
BF–CF #38	Fast	5000	T, DSC
BF–CF #39	Fast	5000	T, DSC
BF–CF #41	Fast	5000	T, DSC
BF–CF #42	Fast	5000	T, DSC
BF–CF #29	Fast	10,000	DSC
BF–CF #47	Fast	10,000	DSC
BF–CF #48	Fast	10,000	DSC
BF–CF #55	Fast	10,000	DSC
BF–CF #57	Fast	10,000	DSC
BF–CF #64	Fast	10,000	DSC
BF–CF #65	Fast	10,000	DSC
BF–CF #40	Fast	180,000	DSC
BF–CF #66	Fast	180,000	DSC
BF–CF #67	Fast	180,000	DSC
BF–CF #43	Slow	5000	T, DSC
BF–CF #50	Slow	5000	T, DSC
BF–CF #51	Slow	5000	T, DSC
BF–CF #52	Slow	5000	T, DSC
BF–CF #53	Slow	5000	T, DSC

BF: boron fiber; CF: carbon fiber; T: tensile test; DSC: differential scanning calorimetry.

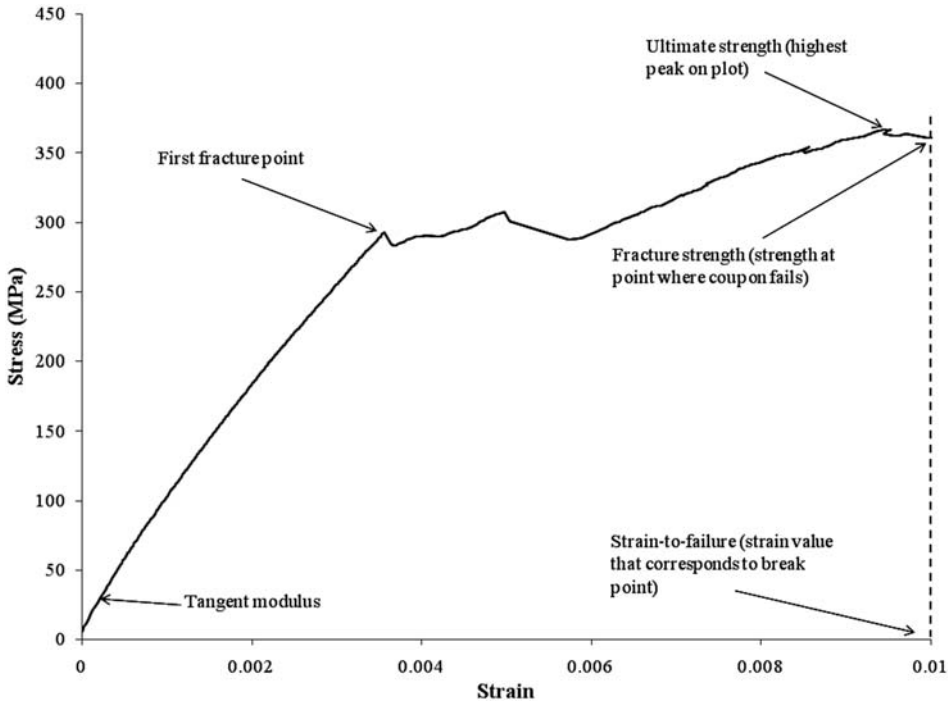

Figure 3. A representative stress-strain curve resulting from a tensile test of an irradiated coupon. From the data, the following quantities are gathered: modulus, ultimate strength, fracture strength, and first fracture point.

each heat cycle were plotted. The T_g was calculated for each sample from the second heat, averaged according to dose and dose rate and compared to the average T_g for the same panels prior to radiation exposure.

In a previous study, identical composite panels were irradiated with 200 MeV protons to a total dose of 5000 Gy (500 krad). FTIR scans via the attenuated total reflectance (ATR) method were acquired from the center of the sample before radiation and immediately after returning from radiation. After the post-irradiation FTIR scans, identical tensile coupons were made and pulled. Post-tensile testing and scanning electron micrographs (SEMs) of the tensile coupons were obtained. SEM samples were mounted on metallic plates with carbon tape to limit charging of the epoxy. The FTIR scans and SEM micrographs obtained from the previous study are discussed and compared with the data gathered from the tensile and DSC tests in this study to provide a more complete discussion.

Results

Tensile test

Load and strain data were collected on 18 tensile coupons, including eight control coupons, five coupons exposed to proton radiation at a fast dose rate and total dose of 5000 Gy and five coupons exposed to proton radiation at a slow dose rate and a total dose of 5000 Gy. With the exception of the control coupons, each coupon was taken from a different panel to account for panel variation. Of the eight control coupons, five were prepared from separate panels and three were cut from the same panel (panel #63 as documented in Table 1). The resulting stress–strain curves of representative coupons (for clarity) of each exposure group are shown in Figure 4. These curves were created by plotting the strain data collected from the strain gage on the coupon versus the calculated stress (ASTM-D-3039) resulting from the load during the tensile test. In Figure 4, the graphs do not start at zero stress and zero strain because of slack in the test setup. Thus, a slack correction algorithm was used on the stress–strain data to produce more accurate calculations of tensile properties. In general, the representative stress–strain results show a trend of lower overall strengths and increased strain to failure with radiation exposure.

Subsequently, the modulus (Figure 5), ultimate strength (Figure 5), fracture strength (Figure 5), strain-to-failure (Figure 6), fracture energy (Figure 6) and first fracture point (Figure 7) were calculated. In Figures 5 and 6 the individual data points are plotted. To show clarity and significance in the first fracture point data (Figure 7), the values from each coupon were averaged for each group, and the standard deviation of the group was calculated. The results are shown in Figures 5 to 7.

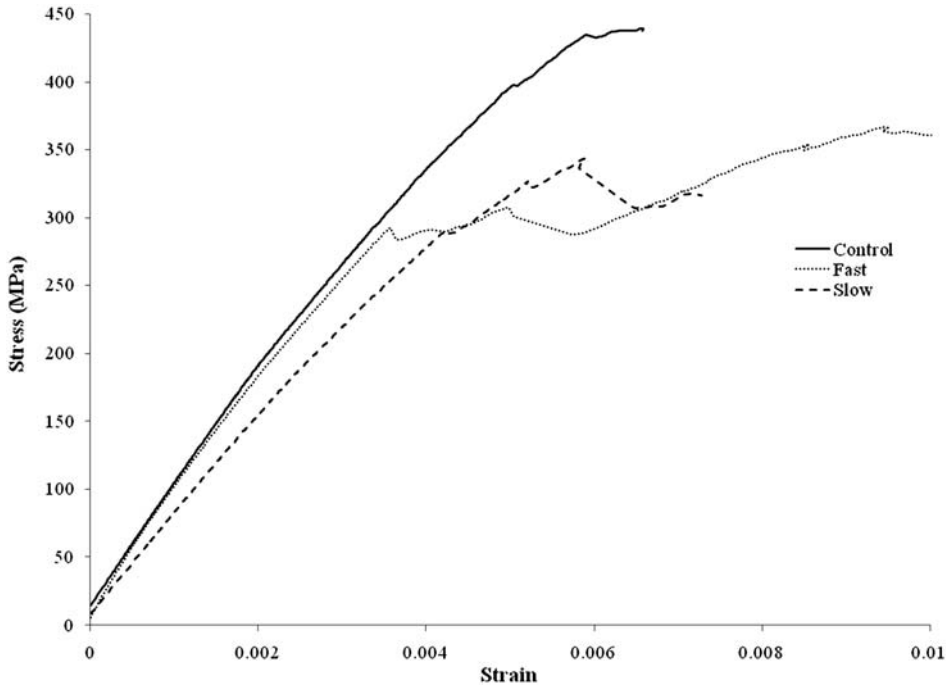

Figure 4. Stress versus strain curve for one representative coupon of the control group, fast group, and slow group.

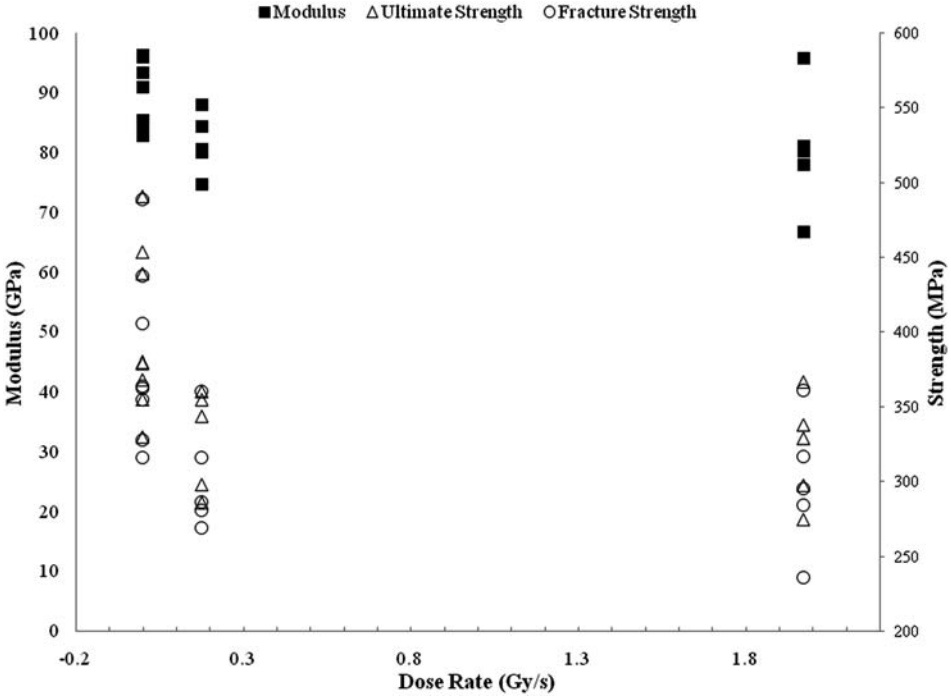

Figure 5. Calculated modulus (■ - left side), ultimate strength (△ - right side), and fracture strength (◯ - right side) for each coupon investigated and plotted against the dose rate exposure.

In Figure 5, the modulus, ultimate strength and fracture strength values generally decreased after irradiation compared to the control, but the scatter amongst the data preclude any definitive conclusions. Potential sources of the error are edge effects resulting from non-standard coupon sizes. However, values for the first fracture point (Figure 7) for the irradiated samples did show significant decrease when compared with

the control. These results show that the material strength decreased with increasing radiation exposure. Furthermore, the values for strain-to-failure and fracture energy of the irradiated samples increased compared with the control, albeit with scatter amongst the data (Figure 6). These data show that after radiation exposure, the strain-to-failure increased and the total fracture energy increased, indicating that the

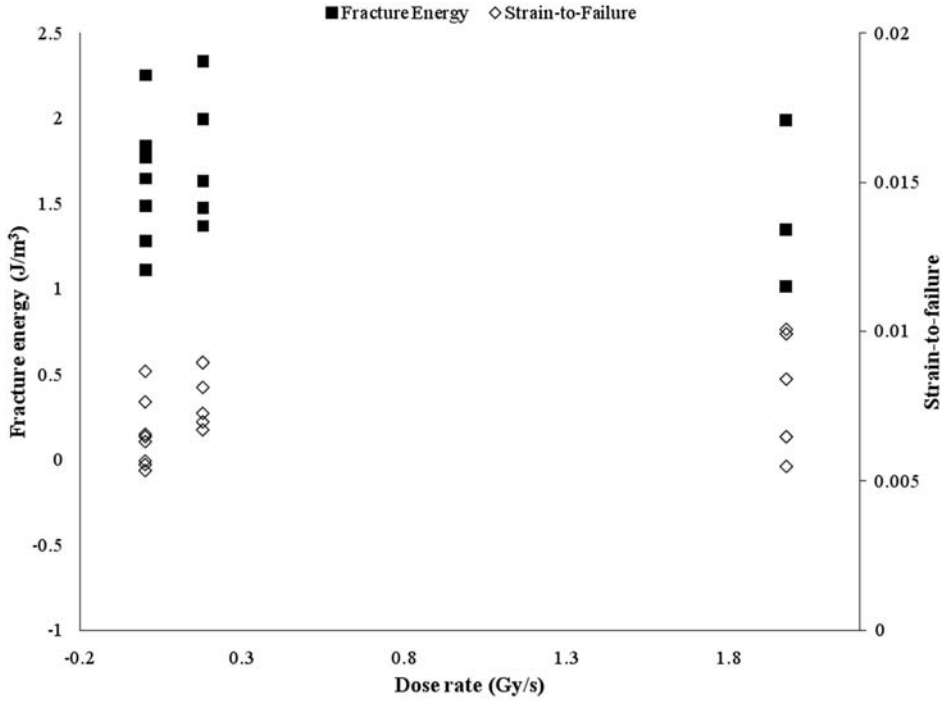

Figure 6. Calculated fracture energy (■ - left side) and strain-to-failure (◇ - right side) for each coupon investigated and plotted against the dose rate exposure.

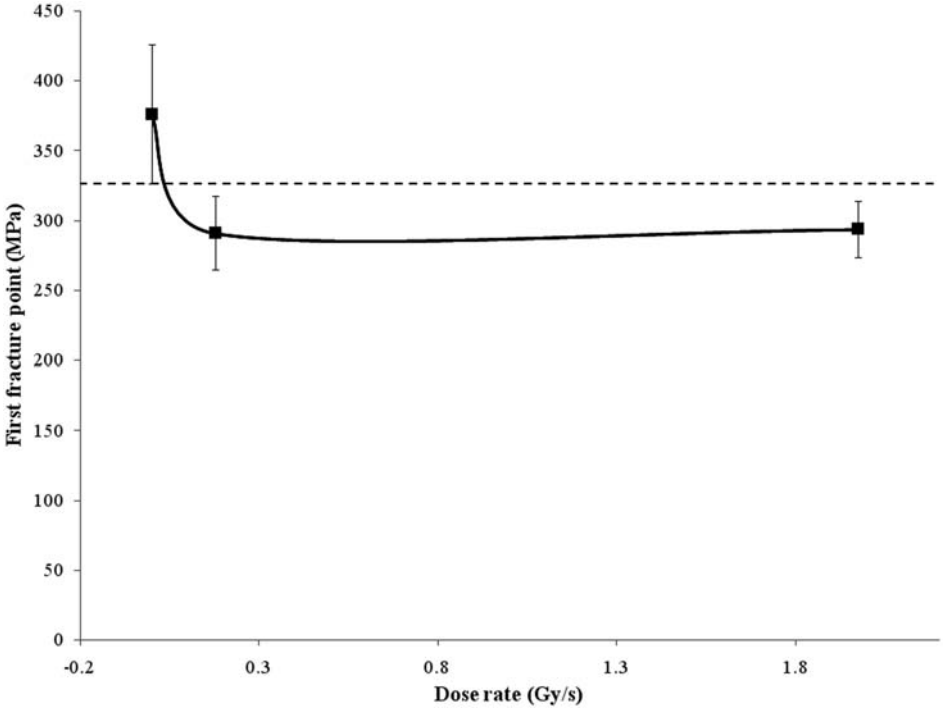

Figure 7. Averaged first fracture point data for the dose rates investigated.

material became tougher. In Figures 5 to 7, there is negligible difference between samples irradiated at a slow dose rate and those irradiated at a fast dose rate. Therefore, no inferences can be made regarding dose effects on tensile properties of this material.

FTIR spectroscopy

Previously, 10 BF–CF panels were investigated with FTIR prior to radiation exposure and immediately after returning from irradiation. The center of the panel was scanned using the ATR method. A background spectrum was obtained prior to characterizing any of the panels and this background spectrum was subtracted from the panel spectrum to remove artifacts, such as water, from the panel spectrum. The baseline was corrected and the scans were smoothed. Of the two irradiation groups, there were seven panels investigated for the slow irradiation and three panels investigated for the fast irradiation. An average of all ten panel scans pre-radiation is shown in Figure 8. The scans from pre- and post-radiation were averaged according to their exposure group, and the averaged scans were subtracted (post−pre) to highlight peaks that had changed with irradiation. The averaged and subtracted scans for both the fast and slow exposure groups are shown in Figure 9, and several peak regions are identified.

In general, with radiation exposure, many of the peaks increased in absorbance. In addition, the panels that underwent fast exposures exhibited greater absorbance values for the peaks than the slow exposure, although the differences were relatively small (~20%, with carbonyl the highest at 35%).

Differential scanning calorimetry

All irradiated samples were characterized via DSC. Two samples from each panel were analyzed prior to radiation exposure, and two samples were analyzed from each panel after radiation exposure. Table 2 shows the dose groups considered for the fast dose rate and the averaged values of the T_g before and after radiation exposure.

An example of the first and second heat of a pre-exposure DSC experiment is shown in Figure 10. The DSC scan followed a heat–cool–heat cycle. The first heat was used to determine if the sample was fully crosslinked from the curing process by confirming the absence of any further cure peaks. The second heat was used to calculate the T_g since the first heat could contain thermal history from the cure. Figure 10 shows the absence of a cure peak in the first heat, indicating a fully crosslinked material, and that the T_g for this sample as determined from the second heat is 128° C. These same features (fully crosslinked samples post-

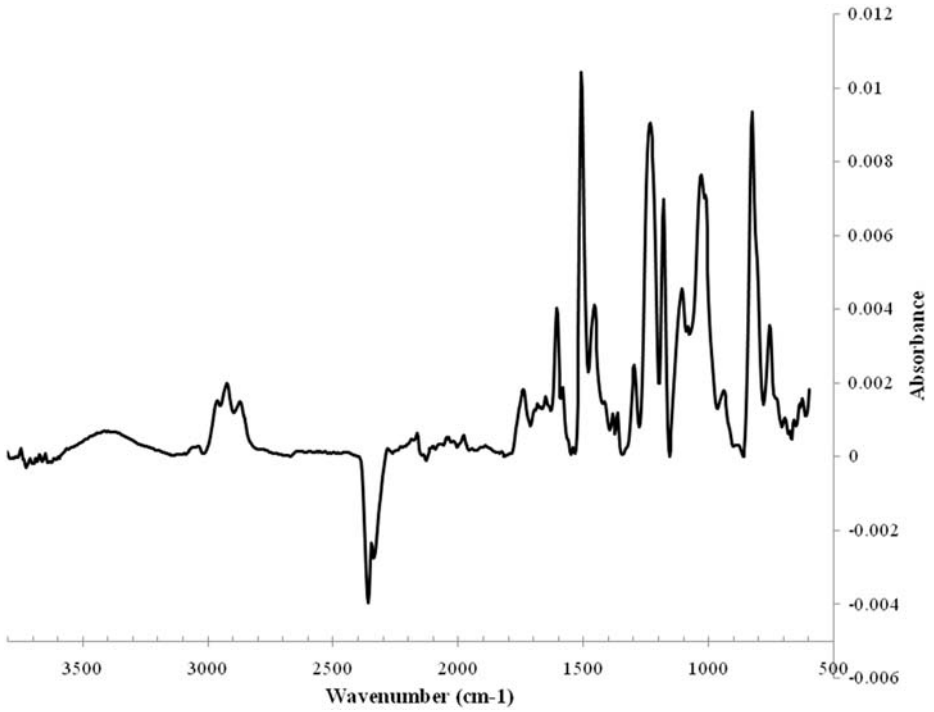

Figure 8. Averaged pre-radiation FTIR spectrum of all ten BF-CF samples scanned with FTIR prior to being exposed to radiation.

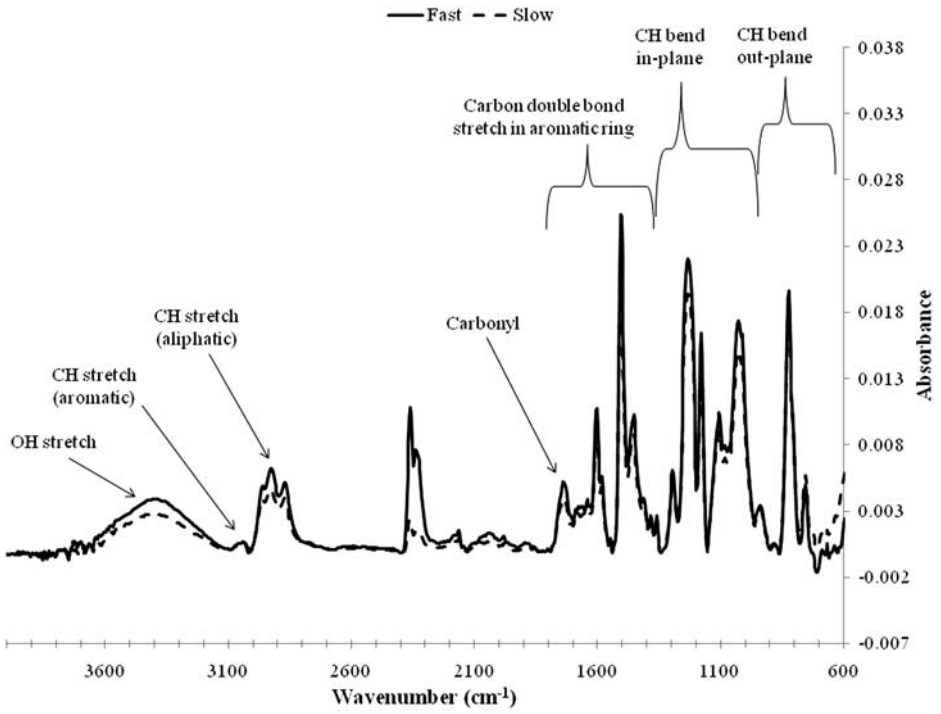

Figure 9. FTIR-averaged scans of the center locations for fast (—) and slow (- - -) exposures where the averaged pre-irradiation scan is subtracted from the averaged post-irradiation scan.
FTIR: Fourier transform infrared.

Table 2. Averaged pre-radiation and post-radiation glass transition temperature values for each dose group evaluated.

Dose		Average (° C)	
Gy	krad	Pre	Post
1000	100	120.35	122.44
5000	500	126.03	123.57
10,000	1000	125.52	121.52
180,000	18,000	134.40	119.69

curing and evidence of a T_g during the second heat) were evident in all samples characterized.

From these graphs, the glass transition temperature was calculated for each sample. The repeat measurements from each sample were averaged and the percent change in the T_g from before radiation exposure to after radiation exposure was calculated. Finally, the percent change was averaged according to total dose and plotted against that dose (Figure 11).

At a very low dose, there appeared to be a small increase in the T_g, but with increasing dose, the T_g of the samples decreased. Further analysis (Table 3) using a paired two sample for means t-test showed that the 1,000 Gy case did not have a sufficient change in the T_g to determine that the radiation dose caused a change in the material. However, with the 5,000 Gy, 10,000 Gy, and 180,000 Gy cases, the analysis showed that at a 0.05 confidence level, the data show that T_g decreases after radiation exposure.

Decreasing T_g values with radiation exposure indicates that chain scission increases with radiation dose. Similar effects were reported in[15,16] and one report concluded that scission predominates when the material is fully crosslinked.[15] The lack of any cure peaks in the DSC data (Figure 10) indicate that the samples were fully crosslinked before radiation. Thus, chain scission in the epoxy is expected with increased radiation exposure.[15]

Furthermore, previous work has shown an empirical correlation (equation (1)) between T_g and the degree of crosslinking.[17–20]

$$M_c = \left(3.9\times10^4\right)/\left(T_g - T_{go}\right) \quad (1)$$

In this equation M_c is the number average molecular weight between crosslinks, T_g is the glass transition temperature and T_{g0} is the glass transition temperature of the pre-cured epoxy. As the glass transition temperature decreases, the molecular weight between crosslinks increases, indicating a degradation of the epoxy network structure.

For the panels irradiated at a total dose of 5000 Gy (500 krad), the T_g for the fast dose rate was

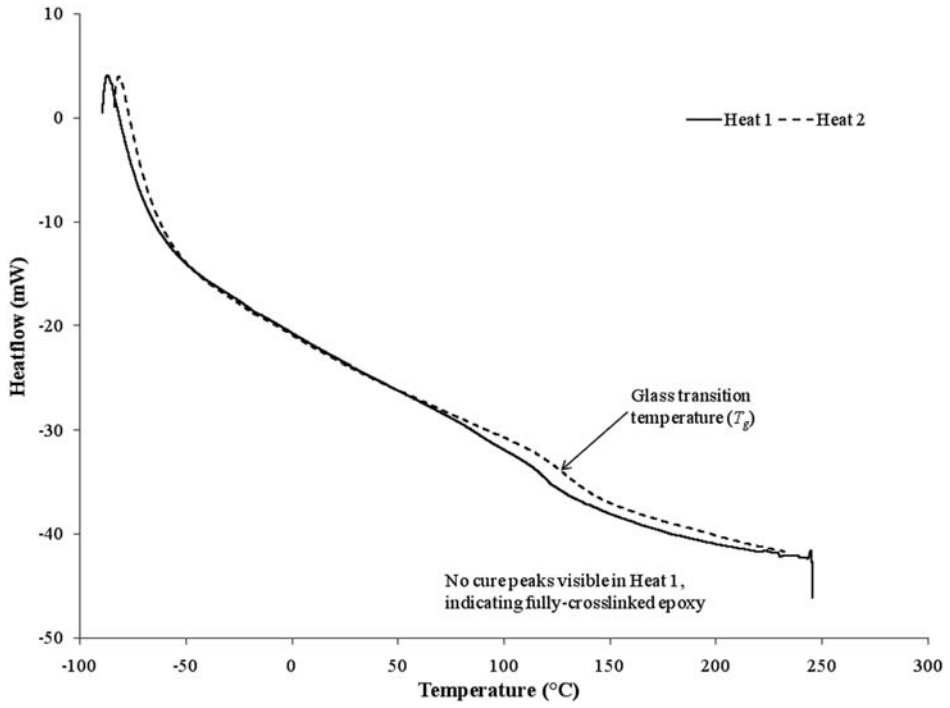

Figure 10. Example of DSC curve for a sample before radiation exposure (BF–CF #22).
BF: boron fiber; CF: carbon fiber; DSC: differential scanning calorimetry.

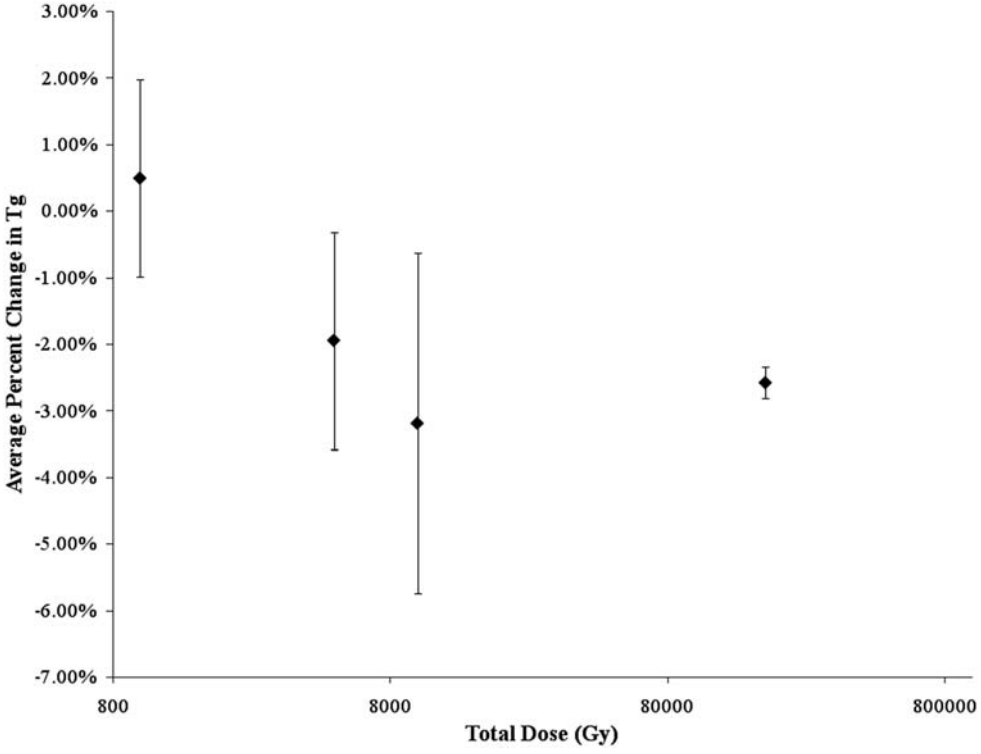

Figure 11. Average percent change in glass transition temperature for each exposure group evaluated.

Table 3. Paired two sample for means *t*-test on the glass transition temperature for the four dose cases evaluated.

	1000 Gy		5000 Gy		10,000 Gy		180,000 Gy	
	Pre-radiation	Post-radiation	Pre-radiation	Post-radiation	Pre-radiation	Post-radiation	Pre-radiation	Post-radiation
Mean	121.79	122.44	126.03	123.57	125.52	121.52	122.86	119.69
Variance	37.20	63.00	6.67	7.16	12.53	19.88	39.32	33.85
t Stat.	−0.50		2.70		3.30		12.05	
$p(T<=t)$ one-tail	0.352		0.027		0.008		0.003	

Table 4. A comparison of the percent change in glass transition temperature for the samples irradiated to 5,000 Gy at fast and slow dose rates.

	Average	Percent change
Fast (pre)	126.03	−1.95
Fast (post)	123.574	
Slow (pre)	128.168	−2.43
Slow (post)	125.056	

compared to the slow dose rate. The results are shown in Table 4.

As shown in the table, the slow dose rate caused a slightly larger depression of the T_g than is observed in the fast dose rate. Thus, it follows logically that samples exposed at a slow dose rate experienced slightly more chain scission than samples receiving radiation at a fast dose rate.

Scanning electron microscopy

Tensile coupons were investigated via scanning electron microscopy. Control coupons without radiation exposure (Figure 12) were compared with coupons exposed to 5000 Gy (500 krad) of 200 MeV protons (Figure 13). In these images, only the boron fibers are shown, as the carbon fibers were in the interior of the coupon and difficult to image without pulling apart the layers of the coupon, essentially destroying the tensile coupon.

In Figure 12, boron fibers in various control samples (i.e. no radiation exposure) are shown. The fibers are covered with attached matrix indicating strong adhesion between the boron fibers and the matrix. Conversely, in Figure 13, after 5000 Gy (500 krad) irradiation, the boron fibers are relatively clear of resin, indicating a weakened fiber-matrix interface bond. In the irradiated panels, clean boron fibers were not widespread throughout the samples. Rather there were instances of clean boron fibers with a majority of the panel showing resin attached to boron fibers. However, the absence of clean boron fibers in the control panels indicates that the change in adhesion of resin to the boron fibers is a result of the radiation exposure.

Discussion

Previous studies of radiation effects on polymeric materials have generally shown one of two effects on the mechanical properties of these types of materials. In some cases, the material shows increased strength and reduced ductility with radiation exposure, and this is generally attributed to increased crosslinking.[3,4,21,22] In other cases, decreased strength is observed and this is attributed to chain scission in the polymer backbone.[21,23–26] These two mechanisms are considered below in the interpretation of the current results on the composite system under consideration.

Composite durability

The decrease in material strength, increase in matrix ductility and decrease in T_g can be attributed to scission effects in the matrix. In other material studies,[15,16,21,22,27] similar degradation was reported and attributed to chain scission as the primary degradation mechanism. The epoxy chemistry typically determines whether the matrix will undergo scission or crosslinking (or both). For instance, in two studies,[21,24] several different types of chemistry are discussed with regard to radiation effects. If the epoxy contains tertiary carbons, these carbons will undergo chain scission most readily, followed by secondary bonded then primary bonded carbons. This hierarchy is due to the dissociation energies of these bonds. The epoxy system used in the present system is a typical aerospace epoxy formulation with toughening agents. One of the most common aerospace epoxy bases is diglycidyl ether of bisphenol-A (DGEBA).[21,24] Comparison of the FTIR spectra of the control BF–CF composite surface (Figure 8) with the FTIR spectra of DGEBA (Figure 14)[28] shows several similarities, such as the aliphatic C–H stretch peaks at $\sim$3000 cm^{-1} the carbon double bond from the

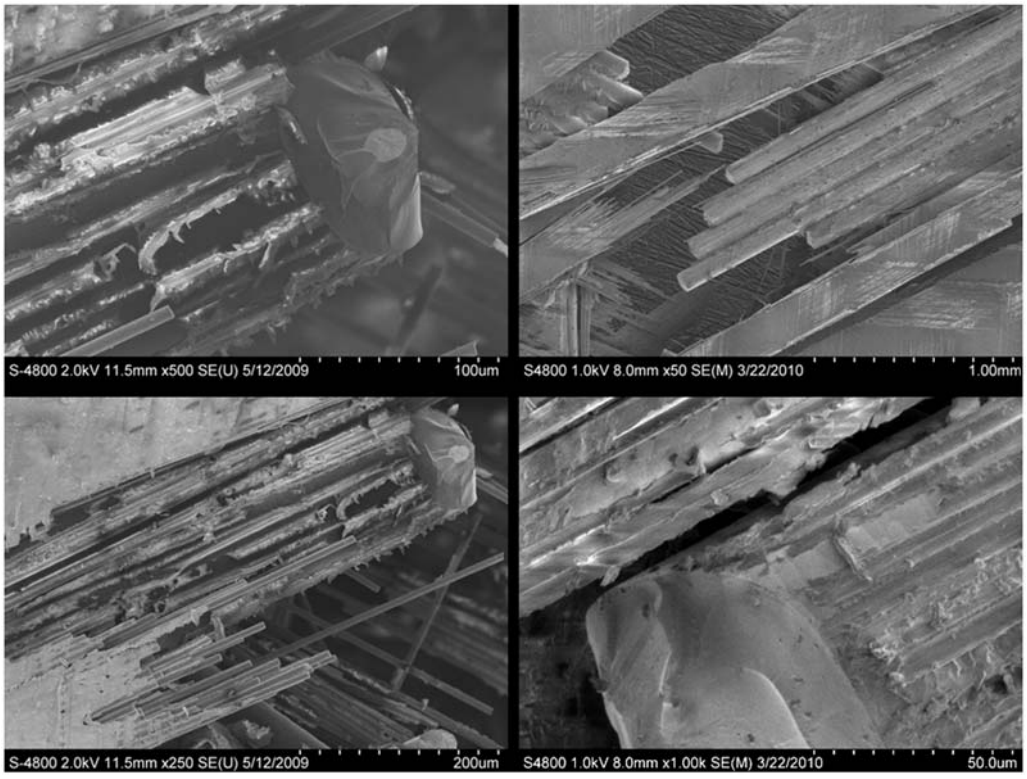

Figure 12. Several scanning electron micrographs of tensile coupons post-fracture that were not exposed to radiation.

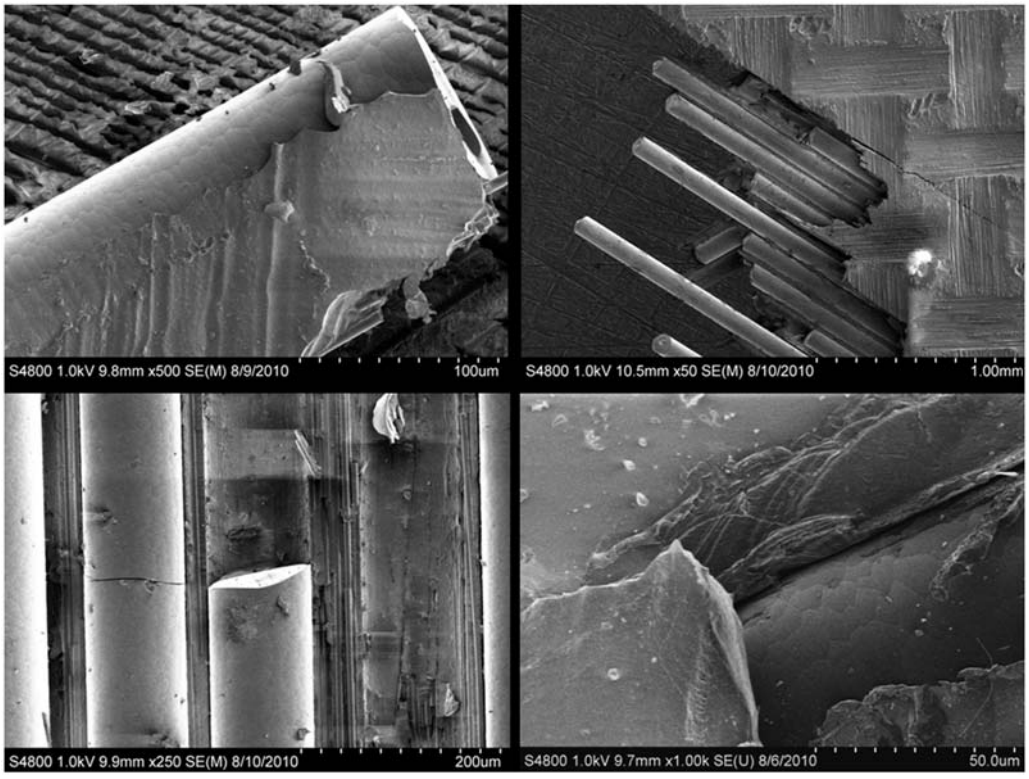

Figure 13. Several scanning electron micrographs of tensile coupons post-fracture that were exposed to 200 MeV protons to a total dose of 5000 Gy (500 krad). The bottom right micrograph shows the interface between a boron fiber and the epoxy.

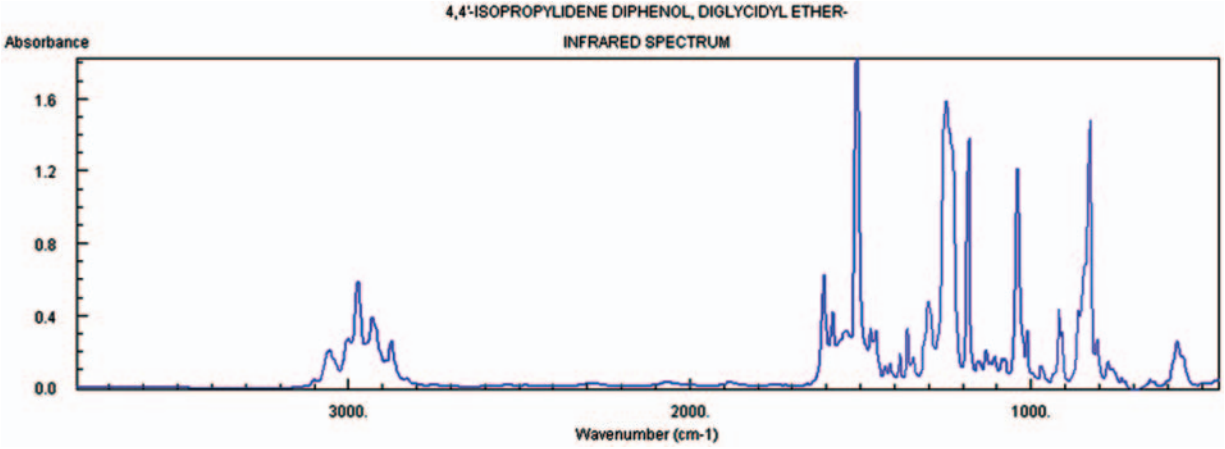

Figure 14. IR spectrum of DGEBA.[27]

aromatic ring at ~1500 cm^{-1}, the C–H bend-in-plane at ~1250 cm^{-1} and the C–H bend out-of-plane at ~850 cm^{-1}. Thus, we can assume that the BF–CF epoxy is based on a DGEBA formulation with toughening agents.

DGEBA contains tertiary carbons, and thus is susceptible to scission during irradiation. However, epoxies also contain aromatic rings that increase resistance to radiation effects by absorbing and dissipating excitation energy.[29] Woods and Pikaev[29] report that the aromatic groups dissipate much of the energy that is absorbed during these tertiary carbon bond cleavages because the product yields in aromatic structures of this nature tend to be lower than one would expect. The efficiency with which the aromatic group can dissipate the energy decreases when the site of energy absorption is farther from the aromatic group.

The FTIR spectra (Figure 9) includes peaks indicative of aromatic features in the epoxy at 3050 cm^{-1} (C–H stretch in the aromatic ring), 1300–1550 cm^{-1} (carbon double bond stretch in the aromatic ring) and 700–900 cm^{-1} (C–H bend out-of-plane).[30] With radiation exposure, the strength of these peaks increased, indicating an increase in aromaticity. However, aromatic structures are less durable when the epoxy is irradiated in the presence of oxygen, often causing oxidation, and many epoxies tend to undergo chain scission under such conditions. Indication of oxidation in an epoxy[26,31] appears as an increase in the absorbance of the carbonyl region (1750 cm^{-1}) and in the hydroxyl region (3300 cm^{-1}). In the BF–CF composite, there is an increase in the absorbance of both of these regions, indicating oxidative degradation. However, studies have shown that the oxidation occurring in epoxies is generally limited to near-surface regions (<20 μm) due to low oxygen diffusion through the material.[26,31] Thus, any oxidation that occurred in the BF–CF composite is likely to be limited to the near-surface regions and have negligible effects on the mechanical properties. Furthermore, when epoxies undergo chain scission because of radiation, the chain scission increases the molecular mobility, further enhancing radical recombination. Through FTIR scans, scission can be observed through increases in aliphatic groups, such as the aliphatic C–H stretch region (2800–3000 cm^{-1}). In Figure 9, increases in absorbance of the C–H stretch region are visible, suggesting an increase in aliphatic groups after radiation as well. Given that the FTIR data show increases in absorbance of all of these regions (aromatic, oxidation and aliphatic), we conclude that competing processes occur in this material, making it difficult to ascertain which process is dominant. While the aromatic groups increased after radiation, there are also increases in areas that indicate oxidation and enhanced scission. Coupling this with the trends shown in the tensile and DSC data, the results suggest that scission is the dominant process, given that oxidation would affect only near-surface regions and would not affect the tensile properties or DSC results.

Toughening

The role of the toughening agent on degradation of the BF–CF composite is worthy of consideration. Toughening agents are added to epoxies to increase fracture toughness and damage tolerance.[5–7] In aerospace composites, thermoplastic additives such as polyethersulfone (PES), a high-temperature thermoplastic, are commonly used.[32,33] In these studies, the amount of toughening is generally in the 10–20 wt% range. However, during radiation exposure PES reportedly undergoes chain scission,[34,35] decreasing tensile strength and T_g. The BF–CF composite is a toughened epoxy, and chain scission of the PES toughening agent may contribute to the observed degradation in material properties.

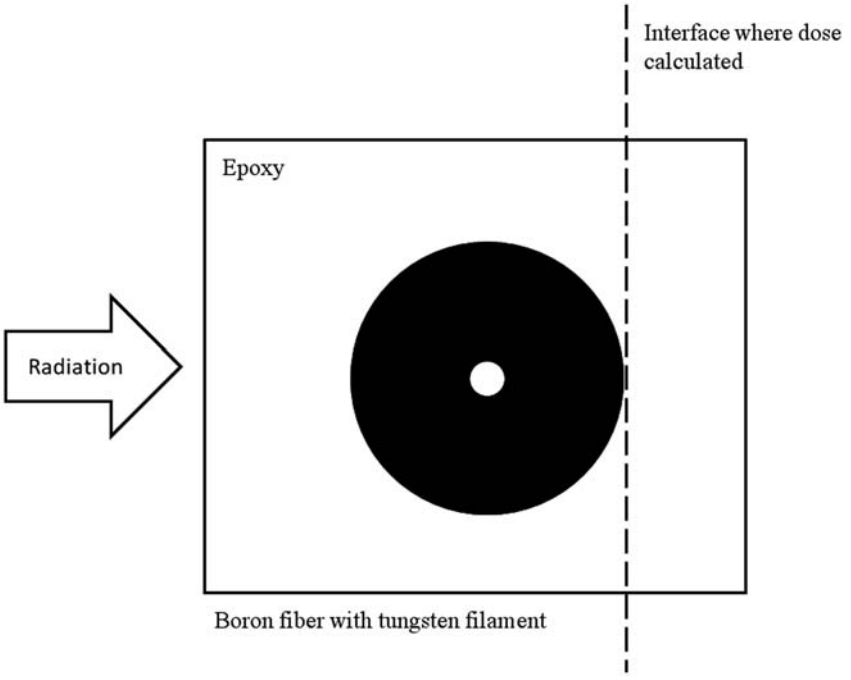

Figure 15. Model of the composite for HZETRN dose calculations at the interface of the boron fiber and the epoxy.

Dose rate effects

One of the compromises made in this study was an increase in the speed of the dose rate in order to perform the experiment within budget and time limitations. To achieve the dose rate experienced during an SPE (~4.63 E-4 Gy/s) would require ~125 days to reach the 5000 Gy dose being investigated in this study. Therefore, we selected a faster dose rate of 1.973 Gy/s (fast dose rate) as well as a slower dose rate (0.177 Gy/s) to investigate possible dose rate effects.

The tensile data showed no significant effects of dose rate, although the DSC data revealed a slightly larger decrease in T_g for the slow dose rate. Dose rate effects, especially in the presence of oxygen, are typically manifested as additional scission occurring as a result of oxidation.[12,36,37] However, in the FTIR data, it is observed that the slow dose rate difference spectrum exhibited slightly reduced peaks when compared with that of the fast dose rate. The FTIR data suggest that less oxidative degradation, scission effects and aromaticity occurred at the slow dose rate as compared to the fast dose rate. However, the differences are minor, and there is insufficient evidence to support dose rate effects occurring in this study.

Aging

Tensile tests were performed four months after radiation exposure, and the indications of composite degradation at these low doses might result from enhanced aging initiated by the radiation exposure. Prior studies showed that radiation exposure of a diglycidyl ether of bisphenol-A/triethylene tetramine (DGEBA/TETA) epoxy system incurs chain scission with radiation exposure if the system is fully crosslinked before radiation exposure.[15,16] Chain scission enhances the molecular mobility, and three months after radiation exposure, the aging kinetics of the epoxy system is accelerated. The results shown in our study do not provide enough information to ascertain whether accelerated aging is in fact occurring in these materials. Further experiments should be undertaken to investigate the mechanical properties at various lengths of time after irradiation and compared with control properties at the same lengths of time to determine whether accelerated aging is occurring in the material.

Fiber debonding

The SEMs of damaged tensile coupons after radiation exposure provided evidence of interface degradation. Previous studies[38,39] have shown the effects of irradiated composites composed of fibers with borated material, including fiber–matrix interface debonding, and the debonding was attributed to increased radiation in the epoxy. The effect was compounded by enhanced secondary radiation at interfaces induced by the primary radiation interaction with the boron.

To investigate the effects of doses the BF–CF/semi-toughened epoxy material might experience at the fiber–matrix interface, a simulation was conducted using the

Table 5. Comparison of the total dose calculated at the interface of a boron fiber and the epoxy with the total dose at the same location in epoxy only. These calculations were done through a simulation using HZETRN.

	Composite (cGy)	Epoxy Only (cGy)	% increase
Dose at Interface	20,583.59	16,760.40	22.81%

HZETRN software.[40,41] In this simulation, the composite was modeled after an SEM image (Figure 15), and the environment used was the October 1989 SPE.

The dose at the interface in the model was compared with the dose at the same location in unreinforced epoxy. The results (Table 5) show that for the October 1989 SPE environment, the boron fiber increases the radiation dose by about 23% compared to a neat epoxy as a result of enhanced secondary radiation production from the boron.

The magnified dose at the interface adds to the enhanced degradation observed in this study. However, given that the debonding of the resin to the fiber was not widespread throughout the samples, a large macroscopic effect as a result of the debonding is not expected. Rather, the debonding of the boron fibers from the resin could be a contributor to the weakened tensile properties observed.

Conclusions

The present study is focused on doses a habitat material might experience during a lunar mission (~5000 Gy or 500 krad). The selected dose is well below that of other studies,[3,4,17,21,42] which typically involved doses on the order of 10^6 Gy (10^8 rad) before significant effects were observed. Given the low doses evaluated in this study compared to other studies, it is not surprising that the effects are minimal. However, most previous studies were performed with low energy gamma radiation or electron radiation, and few, if any, studies involved proton radiation at high energies. In addition, previous studies generally involved pure epoxy composites, whereas the present study focused on toughened epoxy composites. Both factors – high-energy proton radiation and toughened epoxy composites – distinguish the present study from earlier work.

It is concluded that radiation exposure of a BF–CF/semi-toughened epoxy system degrades due to chain scission within the polymer network and subsequent debonding of the resin from the boron fibers when exposed to 200 MeV protons in an oxygenated environment. The factors that lead to and enhance the scission effects are the chemical composition of the epoxy, the presence of toughening agents that are susceptible to radiation damage and potentially enhanced aging and expected increased radiation dose at the interface between the boron fiber and the epoxy. There was some evidence of oxidative degradation at the sample surface, but due to low oxygen diffusion through the sample, the oxidation is not expected to affect bulk properties such as T_g or tensile strength. While most of the tensile results were inconclusive, the first fracture point in the tensile data is significant evidence of the scission effects and may be used as a sensitive initial indicator of composite degradation due to this type of radiation damage. Furthermore, the DSC results showed evidence of decreased T_g with radiation exposure, providing further evidence of scission effects in the composite. There was no evidence of dose rate effects.

In this study, the radiation exposure was accelerated to resemble a 30-year mission, although the conditioning included only radiation, unlike a true space mission. To accurately simulate a long-term space mission, it is necessary to also assess the aging of this material in conjunction with the radiation exposure, especially since there is evidence that radiation causes accelerated aging of such materials. The lifetime and safety ratings of these materials could be impacted as a result of this information and therefore is critical for use of these composites in the deep-space environment.

Acknowledgments

The authors would like to thank Specialty Materials, Inc., for providing the composite materials used in this study and for providing guidance with respect to working with this material. We would like to express our gratitude to the Indiana University Cyclotron Facility, NASA-JSC's Avionics Command and Data Handling Branch, NASA-JSC's Materials and Processes Branch and University of Southern California Department of Chemical Engineering and Materials Science for their continued support in this study and the use of their equipment, facilities and personnel to perform the work.

Conflict of interest

None declared.

Funding

This research received no specific grant from any funding agency in the public, commercial or not-for-profit sectors.

References

1. Milkovich SM, Herakovich CT and Sykes GF. Space radiation effects on the thermo-mechanical behavior of graphite-epoxy composites. *J Compos Mater* 1986; 20(6): 579–593.
2. Leung CL. Space Environmental Effects on Graphite/Epoxy Composites.In: Adsit NR (Ed) *Composites for*

Extreme Environments, ASTM STP 768. American Society for Testing and Materials, 1982, pp. 110–117.
3. Kurland RM, Thomasson JF and Beggs WC. *Radiation testing of composite materials, Insitu versus ex situ effects*. NASA CR-3475, 1981, 1–109.
4. Coulter DR, Gupta A, Smith MV, et al. The effects of energetic proton Bombardment on polymeric materials: experimental studies and degradation models (NASA-CR-177161), 1986, 1–74.
5. Sela N and Ishai O. Interlaminar fracture toughness and toughening of laminated composite materials: a review. *Composites* 1989; 20(5): 423–435.
6. Bagheri R, Marouf BT and Pearson R. Rubber-toughened epoxies: a critical review. *Polym Rev* 2009; 49(3): 201–225.
7. Mimura K, Ito H and Fujioka H. Toughening of epoxy resin modified with in-situ polymerized thermoplastic polymers. *Polymer* 2001; 42(22): 9223–9233.
8. Liskowsky DR and Seitz WW. *Human integration design handbook*. NASA SP-2010-3407, 2010, 1–1136.
9. Atwell W, Koontz S, Reddell B, et al. Meeting radiation protection requirements and reducing spacecraft mass – A multifunctional materials approach. In: *AIAA space 2010 conference and exposition*, Anaheim, CA, 2010, pp.1–10. Reston, VA: (AIAA).
10. Wilson JW, Badavi FF, Cucinotta FA, et al. HZETRN: *description of a free-space ion and nucleon transport and shielding computer program*. NASA Technical paper 3495, 1995, 1–143.
11. Kudoh H, Celina IM, Malone GM, et al. Pulsed E-beam irradiation of polymers – A comparison of dose rate effects and let effects. *Radiat Phys Chem* 1996; 48(5): 555–562.
12. Clough RL and Gillen KT. Combined environment aging effects: radiation-thermal degradation of polyvinylchloride and polyethylene. *J Polym Sci Part A: Polym Chem* 1981; 19(8): 2041–2051.
13. Alariqi SAS, Singh RP and Rao BSM. γ-Initiated oxidation of isotactic polypropylene: effect of γ-dose rate on durability. *Arab J Sci Eng* 2011; 36(1): 29–38.
14. Von Przewoski, Barbara. (2011). RERS1, Indiana University Cyclotron Facility, http://www.iucf.indiana.edu/rerp/rers1.php, (retrieved November 19, 2012).
15. Davenas J, Stevenson I, Celette N, et al. Stability of polymers under ionising radiation: the many faces of radiation interactions with polymers. *Nucl Instrum Methods Phys Res Sect B* 2002; 191: 653–661.
16. Vignoud L, David L, Sixou B, et al. Influence of electron irradiation on the mobility and on the mechanical properties of DGEBA/TETA Epoxy Resins. *Polymer* 2001; 42: 4657–4665.
17. Sasuga T and Hagiwara M. Disintegration of network structure of bismaleimide-triazine resin by electron beam irradiation. *Polymer* 1986; 27: 681–685.
18. Murayama T and Bell JP. Relation between the network structure and dynamic mechanical properties of a typical amine-cured epoxy polymer. *J Polym Sci Part A-2* 1970; 8: 437–445.
19. Kenyon AS and Nielsen LE. Characterization of network structure of epoxy resins by dynamic mechanical and liquid swelling tests. *J Macromol Sci Pure Appl Chem* 1969; 3(2): 275–295.
20. Nielsen LE. Cross-linking: effect on physical properties of polymers. *J Macromol Sci Rev Macromol Chem Phys* 1969; C3(1): 69–103.
21. Parkinson WW and Sisman O. The use of plastics and elastomers in nuclear radiation. *Nucl Eng Des* 1971; 17: 247–280.
22. Kumar BG, Singh RP and Nakamura T. Degradation of carbon fiber-reinforced epoxy composites by ultraviolet radiation and condensation. *J Compos Mater* 2002; 36(24): 2713–2733.
23. Queiroz DPR, Fraïsse F, Fayolle B, et al. Radiochemical ageing of epoxy coating for nuclear plants. *Radiat Phys Chem* 2010; 79(3): 362–364.
24. Memory JD, Fornes RE and Gilbert RD. Radiation effects on graphite fiber reinforced composites. *J Reinf Plast Compos* 1988; 7(1): 33–65.
25. Dasilva F, Dasaquino K and Araujo E. Effects of gamma irradiation on poly(vinyl chloride)/polystyrene blends: investigation of radiolytic stabilization and miscibility of the mixture. *Polym Degrad Stab* 2008; 93(12): 2199–2203.
26. Longiéras N, Sebban M, Palmas P, et al. Degradation of epoxy resins under high energy electron beam irradiation: radio-oxidation. *Polym Degrad Stab* 2007; 92(12): 2190–2197.
27. Yu G, De-zhuang Y, Jing-dong X, et al. Effect of proton irradiation on mechanical properties of carbon/epoxy composites. *J Spacecr Rockets* 2006; 43(3): 505–508.
28. Linstron PJ and Mallard WG, eds. NIST chemistry webbook. *NIST standard reference database number 69*. National Institute of Standards and Technology, Gaithersburg MD, 20899, http://webbook.nist.gov (retrieved 15 July 2012).
29. Woods RJ and Pikaev AK. *Applied radiation chemistry: radiation processing*. New York, NY: Wiley & Sons, 1994, pp.197–199.
30. Stuart B. *Infrared spectroscopy: fundamentals and applications*. New York, NY: Wiley & Sons, 2004, pp.71–93.
31. Rivaton A, Moreau L and Gardette J-L. Photo-oxidation of phenoxy resins at long and short wavelengths—I. Identification of the photoproducts. *Polym Degrad Stab* 1997; 58(3): 321–332.
32. Hedrick JL, Yilgor I, Jurek M, et al. Chemical modification of matrix resin networks with engineering thermoplastics: 1. Synthesis, morphology, physical behaviour and toughening mechanisms of poly(arylene ether sulphone) modified epoxy networks. *Polymer* 1991; 32(11): 2020–32.
33. Mimura K, Ito H and Fujioka H. Improvement of thermal and mechanical properties by control of morphologies in PES-modified epoxy resins. *Polymer* 2000; 41(12): 4451–4459.
34. Sasuga T, Kawanishi S, Nishii M, et al. Effects of ion irradiation on the mechanical properties of several polymers. *Int J Radiat Appl Instrum Part C Radiat Phys Chem* 1991; 37(1): 135–140.

35. Sasuga T, Kudoh H and Seguchi T. High energy ion irradiation effects on polymer materials – Changes in mechanical properties of PE, PSF and PES. *Polymer* 1999; 40: 5095–5102.
36. Wilski H. The radiation induced degradation of polymers. *Radiat Phys Chem* 1987; 29(1): 1–14.
37. Rivaton A and Arnold J. Structural modifications of polymers under the impact of fast neutrons. *Polym Degrad Stab* 2008; 93(10): 1864–1868.
38. Klabunde CE and Coltman RR Jr. Debonding of epoxy from glass in irradiated laminates. *J Nucl Mater* 1983; 117: 345–350.
39. Egusa S, Kirk MA and Birtcher RC. Neutron irradiation effects on the mechanical properties of organic composite materials. *J Nucl Mater* 1984; 126(2): 152–159.
40. Slaba TC, Blattnig SR, Aghara SK, et al. Coupled neutron transport for HZETRN. *Radiat Meas* 2010; 45(2): 173–182.
41. Slaba TC, Blattnig SR and Badavi FF. Faster and more accurate transport procedures for HZETRN 2010; 1–56.
42. Wolf KW, Memory JD, Gilbert RD, et al. Effects of 0.5-MeV electrons on the interlaminar shear and flexural strength properties of graphite fiber composites. *J Appl Phys* 1983; 54(10): 5558–5582.